3rd European Thermal Sciences Conference 2000
E.W.P. Hane, W. Heidemann and K. Spindler (Editors)

EVAPORATION AND CONDENSATION OF R22 INSIDE TWO MICROFIN TUBES OF NEW DESIGN

A. Muzzio and A. Niro

Dipartimento di Energetica, Politecnico di Milano
piazza Leonardo da Vinci 32, I-20133 Milano, Italy

ABSTRACT

Saturated flow boiling and convective condensation experiments for oil-free refrigerant R22 have been carried out with two microfin tubes of new design, that mainly differ in the number of fins, and with a smooth tube. All the tubes have the same outer diameter of 9.52 mm and are horizontally operated. Data are for mass fluxes ranging from about 90 to 440 kg/s m^2. In boiling tests, the nominal saturation temperature is 5 °C, with inlet quality varying from 0.2 to 0.6 and the quality change ranging from 0.1 to 0.5. In condensation, results are for saturation temperature equal to 35 °C, with inlet quality between 0.8 and 0.4, and quality change within 0.6 and 0.2. The effect of mass flux, heat flux and vapour quality on heat transfer coefficients and pressure drop are examined in the present investigation. The comparison shows a large heat transfer augmentation with a moderate increment of pressure drops, especially in evaporation. In fact, for the microfin tube with the lesser number of fins, the enhancement factor comes up to 4 while the penalty factor is about 1.4 at the most. The increase of the number of fins lowers the heat transfer performance both in evaporation and condensation.

1. INTRODUCTION

Microfin tubes have outstanding performance in enhancing heat transfer for both evaporation and condensation and have been widely used in the air-conditioning and refrigeration industries. Thus, in recent years, many efforts have been spent in designing and developing microfin geometries which could provide high heat transfer coefficients and low pressure drop penalty.

Heat transfer characteristics of microfin tubes have been extensively studied over the past twenty years; detailed literature reviews are presented by Webb [1-2], Thome [3], Kandlikar and Raykoff [4] and Schlager [5]. Several papers, particularly in the first stage of work with microfin tubes, focused on the effects of various geometrical parameters such as tube diameter, spiral angle, fin height and shape, spacing between the fins and the number of fins. However, in spite of the number of published studies, the fluid-dynamic and heat transfer processes involved are so complex that rationally based predictive methods are not available and the reliable evaluation of the performance of microfin tubes remains experimental. Indeed, there is still a large demand of further experimental research in order to test new microfin tubes and refrigerants.

Moved by these reasons, we are currently performing an experimental investigation of flow boiling and convective condensation of halo-carbon refrigerants inside microfin tubes as described in Muzzio et al. [6]. This paper reports on average heat transfer coefficient and pressure drop during evaporation and condensation of oil-free refrigerant R22 in a smooth tube and two microfin tubes with new cross-section profiles. The main difference between microfin tubes consists in the number of fins so that, from the comparison of the performance, the effect of this parameter can be inferred. All the tubes have the same outer diameter of 9.52 mm and are horizontally operated.

2. APPARATUS AND TEST PROCEDURE

The experimental equipment was described in some detail in a previous paper by Muzzio et al. [6] and will, therefore, be covered only briefly here. A simplified schematic diagram of the experimental facility is shown in Figure 1. The rig consists of three circuits, namely, a sealed refrigerant circuit, a water circuit to evaporate or condense the refrigerant in the test section, and a chilled coolant (water-glycol solution) circuit.

The main components of the refrigerant circuit are a boiler, the test section, a condenser, a gear pump and a filter dryer. The boiler is equipped with a heater consisting of three electrical cartridges of 1, 1.5 and 2.5 kW power. Liquid and vapour are drawn from it through two distinct lines; the liquid line is equipped with a subcooler while a superheater is installed on the vapour line. The liquid mass flow rate is measured by a Coriolis flow meter while float-type flow meters are installed on the vapour line. The liquid and vapour flow rates are controlled by precision metering valves. Downstream of the valves, vapour and liquid streams are mixed; the resulting two-phase mixture flows through a 1.5 m long calming section and then enters the test section. At the exit, refrigerant flows through a second calming section (1.8 m) and then is discharged to the condenser, which maintains the test section outlet pressure at a given value. Finally, the refrigerant is drawn from the condenser by a gear pump and is conveyed through a filter dryer to the boiler.

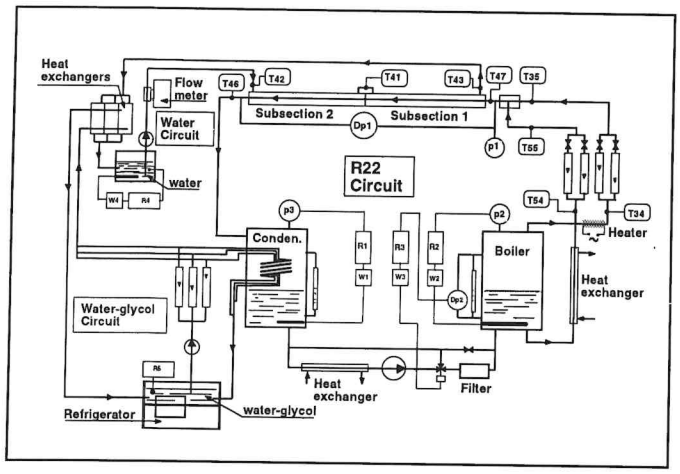

Figure 1. Schematic diagram of the experimental apparatus.

The water loop sets the condition of the water entering the annulus side of the test section. It contains a centrifugal pump that circulates demineralized water, a magnetic flow meter that measures the flow rate, and a combination of a plate heat exchanger and an electrical heater controlling the water temperature. Finally, the chilled coolant circuit is filled with a water-glycol solution and it consists of a commercial refrigeration unit and a centrifugal pump. Such a circuit provides the cold medium circulated in the heat exchangers placed in the refrigerant condenser or mounted on both the refrigerant and the water circuits.

The test section contains the tube undergoing experimental testing. It consists of a double-pipe heat exchanger, divided into two identical subsections, where refrigerant flows inside the inner tube and water flows countercurrently in the outer annulus. The inner tube is made of copper with 9.52 mm o.d and 1.3 m length. The distance between the inlet and discharge ducts of the jacket is 1.12 m which is assumed as the active heat transfer length for the subsection. At the exit of both subsections there is mounted a sight glass made of 80 mm long, 8.5 mm i.d., pyrex smooth tube. These sight glasses are neither heated or cooled. Two pressure-taps are located at the inlet and outlet of the first subsection and at the outlet of the second one, respectively. Both subsections are equipped with four T-type thermocouples to measure wall temperatures. The thermocouples are placed in pairs on the top and at the bottom of the tube and are cemented in longitudinal grooves cut in the outside wall of the tube. Calming and test sections are thermally insulated by a 10 cm thick, glass-wool annulus.

Signals from thermocouples and transducers are cyclically read by a data acquisition unit and sent to an on-line PC. In order for all variables to be affected by similar RMS relative errors, the measurements of refrigerant temperature, pressure drop and water flow rate are based on 30, 50 and 100 readings for cycle, respectively. Every experimental datum, instead, is obtained by averaging the measurements of ten cycles in order to reduce the influence of random errors and fluctuations. Finally, for every operative condition, more than ten experimental data are collected.

The heat transfer coefficient is computed as follows. We assume the refrigerant temperature varies linearly between the value T_{in}, measured at the entrance of the test section, and the value T_{out} computed at the exit as $T_s(p_s(T_{in}) - \Delta p)$, where T_s is the function correlating the saturation temperature to the pressure, p_s the inverse function of T_s, and Δp the pressure drop measured along the test section. Then, for each subsection we calculate the mean refrigerant temperature $T_{r.m,i}$, the mean wall temperature $T_{w.m,i}$, the refrigerant to wall temperature mean difference $\Delta T_{m,i} = (T_{w.m,i} - T_{r.m,i})$, and the heat transfer coefficient $h_i = q_i/\Delta T_{m,i}$ where q_i is the mean heat flux based on a nominal inside area corresponding to the maximum internal diameter, i.e, the diameter at the root of microfins. Eventually, we compute the average heat transfer coefficient for the test section as the arithmetic mean of the subsection coefficients h_i. Relevant variables for the present investigation are affected by the following representative experimental uncertainties measured or estimated by a propagation error analysis: ±2.8% for the refrigerant mass flow rate, ±1.3% for the inlet quality, ±0.2 K between the refrigerant temperature and the saturation one, ±0.03 K between the wall and refrigerant temperatures with the refrigerant trapped in the test section and the water flowing, ±1.0% for the refrigerant pressure drop, ±1.0% for the water volume flow rate, ±0.02 K for the water temperature difference between the subsection inlet and outlet, ±1.4% for the heat rate, and ±7% for the average heat transfer coefficient.

3. RESULTS AND DISCUSSION

In saturated flow boiling or convective condensation, for fixed test section configuration, i.e., dimension and shape of the cross section, length, orientation with respect to gravity, both pressure drop and average heat transfer coefficient depend on four independent variables, namely, total mass flow rate, temperature (or pressure), inlet thermodynamic quality and heat rate. Since quality change along the test section depends linearly on heat rate, a different but equivalent parameterisation can be obtained by substituting the former with the latter quantity in the list of independent variables.

The experimental data reported here were obtained on two microfin tubes of new design developed and manufactured by Trefimetaux, i.e., Metofin 952-30VA40/54A and 952-45HVA 40/82, as well as on a smooth tube. All tubes have the same

Figure 2. Drawing of the microfin cross-section profile.

Parameter	Tube	HVA	VA	Smooth
Outside diameter	[mm]	9.52	9.52	9.52
Maximum inside diameter	[mm]	8.62	8.92	8.92
Bottom wall thickness	[mm]	0.45	0.30	0.30
Higher fin height	[mm]	0.20	0.23	-
Lower fin height	[mm]	0.17	0.16	-
Apex angle		40°	40°	-
Number of grooves		82	54	-
Helix angle		18°	18°	-
Heat transfer internal surface ratio		1.84	1.58	1
Actual cross-section surface ratio		0.946	0.963	1

Table 1. Geometrical parameters of the tested tubes.

outer diameter of 9.52 mm. The microfin tubes tested, which we will denote as tubes VA and HVA respectively, are both characterised by sharp fins (apex angle of 40°) alternating with two different heights. This latter feature distinguishes these tubes from other microfin tubes of new design. A cross-section drawing of the tubes VA and HVA, whose main distinction lies in the fin numbers, is reported in Figure 2, whereas values of their geometric parameters are listed in Table 1 together with dimensions of the smooth tube. This table also lists the heat transfer internal surface ratio and the actual cross-section ratio with respect to the smooth tube.

Evaporation tests were carried out at a nominal saturation temperature of 5 °C (±0.2 K) corresponding to a pressure of 0.58 MPa while, in condensation, the nominal temperature was 35 °C (±0.2 K) corresponding to a pressure of 1.35 MPa. Total mass flow rate, inlet thermodynamic quality and quality change were varied in turn while keeping the others constant, in order to demonstrate clearly the effect of each variable against the others. The total mass flow rate ranged from 5.56 to 25 g/s corresponding to a mass flux G, with respect to a nominal cross-section area based on the maximum internal diameter, that varies between about 90 and 440 kg/sm^2. The inlet quality x_{in} was varied from 0.2 to 0.65 in evaporation, and between 0.9 and 0.4 in condensation; the quality change Δx from 0.1 to 0.7 in evaporation and from 0.2 to 0.8 in condensation.

Figure 3 shows the boiling heat transfer coefficient h_b plotted versus the mass flux G for the tested microfin tubes; data obtained on the smooth tube are also included for comparison. For such data, nominal inlet quality and quality change are x_{in}=0.3 and Δx=0.3, respectively. In considering this figure it is worth keeping in mind that as the mass flux increases at constant Δx an accompanying variation in heat flux sets up. For the data here reported, the average heat flux ranges from about 5.2 to 24 kW/m^2. As expected, the boiling heat transfer coefficient is an increasing function of G, and its values for microfin tubes result much higher than those for the smooth tube, although they are characterised by a lower growth rate. The tube VA appears to have the best performance. Its evaporation enhancement factor -defined as the ratio of the microfin tube heat transfer coefficient to that of the smooth tube - ranges between about 4 and 1.6, with an average increment of 20% with respect to the tube HVA. In both cases, the enhancement factor turns out to be a decreasing function of G. At the high mass flux, the value of the enhancement factor corresponds approximately to the area ratio for the microfin tube VA but it is not so for the tube HVA which displays a lower heat transfer coefficient in spite of a comparatively larger effective heat transfer surface. These results do not conform to the remark by Eckels and Pate [7] who, on the basis of the findings of their experimental studies, concluded that at the high mass flux, the heat transfer increase in the microfin tube is due to the area increase. On the contrary and even at the high mass flux, they support the observation by Ito and Kimura [8] that the increase in boiling heat transfer coefficient cannot be explained simply from an extension of the area.

The effect of average quality x_m on the evaporation heat transfer coefficient, for fixed mass flux and quality change (Δx=0.3), is shown in Figure 4. For G=224 kg/sm^2 (G=238 kg/sm^2 with the HVA tube) the microfin tubes exhibit, in the tested quality range, a continuous increase in the heat transfer coefficient with average quality. On the contrary, at a lower mass flux (G=143 kg/sm^2) with the microfin tube HVA, a distinct maximum in heat transfer coefficient is observed at a high average vapour quality (x_m≈0.75). From a closer inspection of these data it will be also noted that, for x_m below approximately 0.55, there is little effect of the vapour quality on the heat transfer coefficient. However, a further increase in x_m up to the vapour quality at which the peak occurs, results in a substantial increase in h_b. This behaviour may possibly be attributed to the transition from stratified-wavy flow, where the major heat transfer mechanism may be due to nucleate boiling, to annular flow where forced convection type heat transfer is dominant. The preceding remarks are supported by the visual observation of the flow patterns, that showed a shift toward lower vapour qualities of the flow regime transition with increasing mass flux. The fall off in the heat transfer coefficient after the peak is caused by the dryout onset. Heat transfer data relevant to the second subsection, not reported here, indicate that dryout occurs at a vapour quality of approximately 0.9. For the smooth tube, instead, a slightly marked maximum is observed, approximately located at x_m=0.7. Hence, it can be inferred that micro

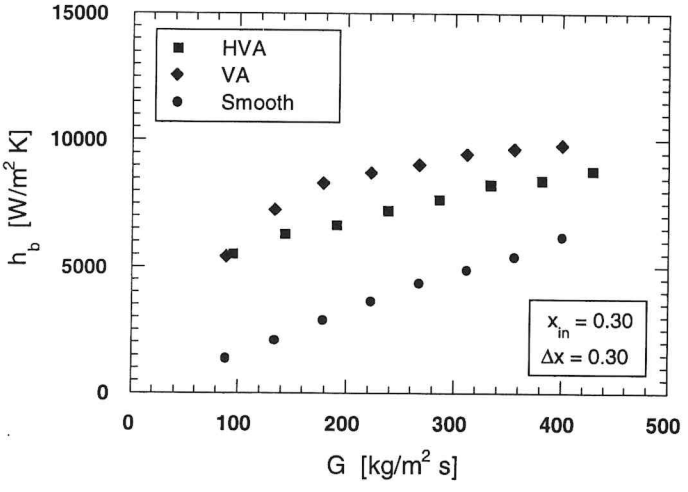

Figure 3. Flow-boiling coefficient h_b versus mass flux G for fixed inlet quality x_{in} and quality change Δx.

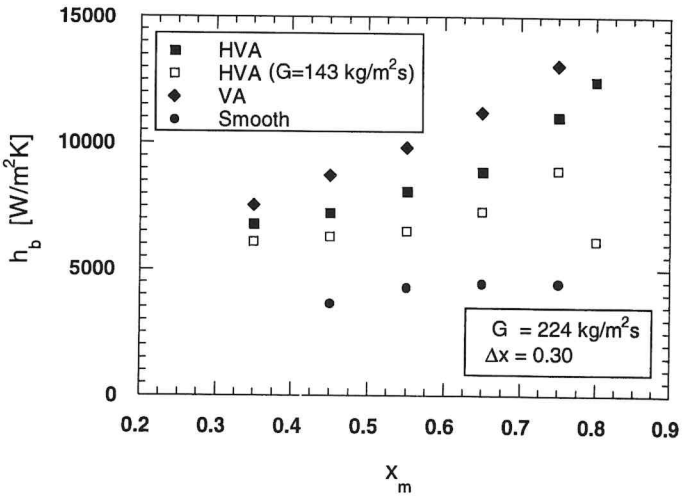

Figure 4. Flow-boiling coefficient h_b versus average quality x_m for fixed mass flux G and quality change Δx.

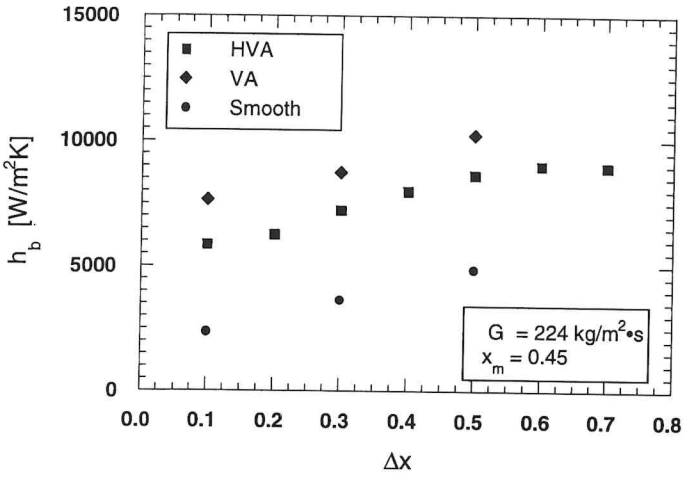

Figure 5. Flow-boiling coefficient h_b versus quality change Δx for fixed mass flux G and average quality x_m.

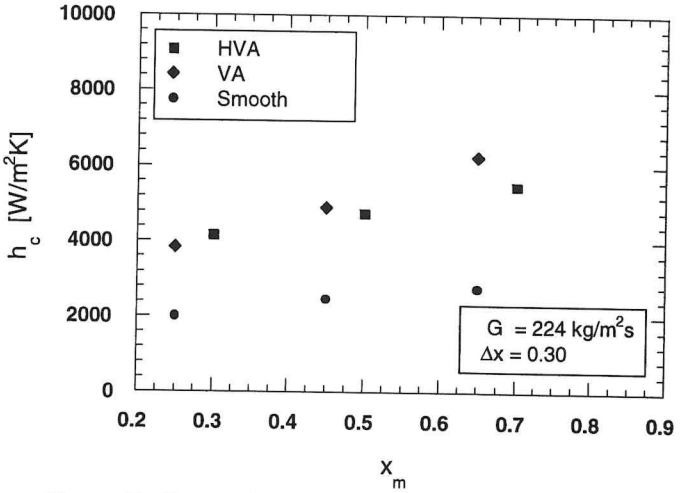

Figure 7. Convective condensation coefficient h_c versus average quality x_m for fixed mass flux and quality change.

finning seems to provide, in addition to the substantial heat transfer enhancement, a shift of the dryout occurrence in the region of higher qualities.

The influence of the quality change (heat flux) for given mass flux and average quality (G=224/238 kg/sm^2 and x_m=0.45) is depicted in Figure 5. Data show that the heat transfer coefficient, in the range of outlet vapour qualities from 0.5 to 0.7, is also an increasing function of Δx for all the tubes with approximately the same growth rate. Values for the tube VA result about 30% higher than those for the tube HVA. However, for the latter tube, the influence of Δx on the heat transfer coefficient grows weaker at higher vapour quality and eventually reverses owing to the onset of dryout. In this respect, it is worth noticing that here dryout is already present at outlet vapour quality of about 0.8, while data reported in Figure 4 at the same mass flux, show that drying does not occur even at outlet vapour quality of 0.95. A possible explanation of this fact resides in the different value of the average heat flux that strongly affects dryout occurrence. In the case where dryout is not present the value of the average heat flux is approximately equal to 17 kW/m^2 while where it occurs the average heat flux amounts to about 33 kW/m^2.

Condensation heat transfer results versus mass flow rate, for fixed inlet and outlet vapour qualities (x_{in}=0.8 and x_{out}=0.2), are shown in Figure 6; for the investigated range of G, the all liquid Reynolds number varies from about 3500 to 16000. As in evaporation, a substantial heat transfer enhancement is achieved by both the microfin tubes with respect to the smooth tube. Again, the tube VA shows the most favourable heat transfer performance; the enhancement factors vary from a maximum of about 2.7 at low mass fluxes to a minimum of 1.8 at high mass fluxes.

Figures 7 and 8 depict the effect on condensation heat transfer coefficient of average quality and quality change, respectively. It is seen that the condensation heat transfer coefficient increases with quality at constant mass flux and quality change (G=224/238 kg/sm^2 and Δx=0.3) for both smooth and microfin tubes. However, the rate of increase is higher for the microfin tubes than for the smooth tube and much higher for the VA tube. On the contrary, the heat transfer coefficient seems to be unaffected by variation in the quality change, at fixed mass flux and average vapour quality.

Figures 9, 10 and 11 present results for the evaporation pressure drop, obtained in the same conditions reported in figures 3, 4 and 5, respectively. For all tubes, pressure drop

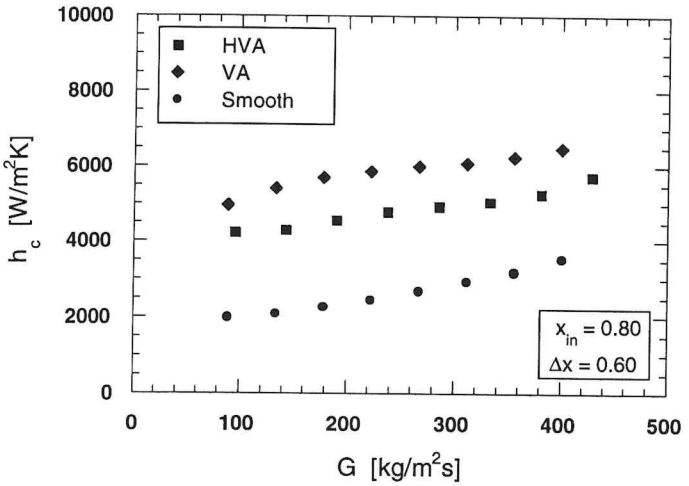

Figure 6. Convective condensation coefficient h_c versus mass flux G for fixed inlet quality x_{in} and quality change Δx.

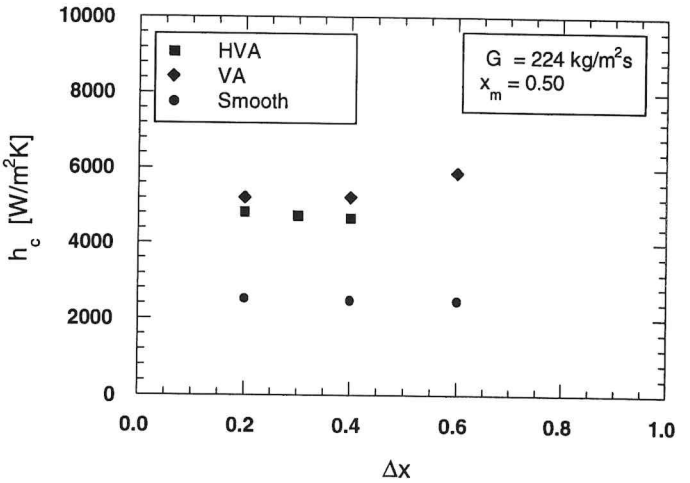

Figure 8. Convective condensation coefficient h_c versus quality change Δx for fixed mass flux and average quality.

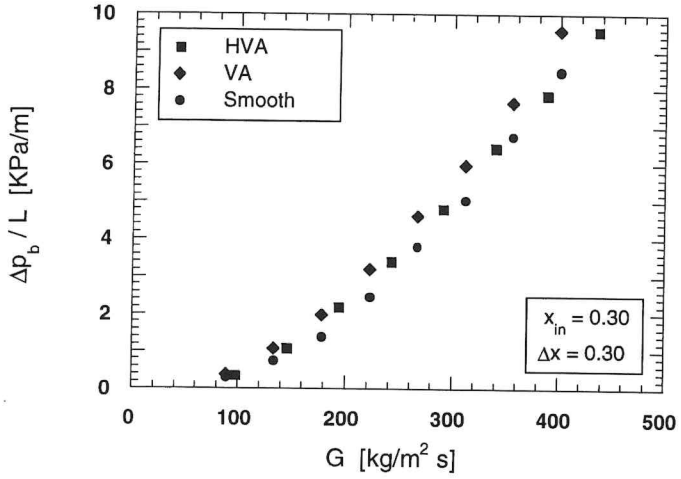

Figure 9. Flow-boiling pressure drop $\Delta p_b/L$ versus mass flux G for fixed inlet quality x_{in} and quality change Δx.

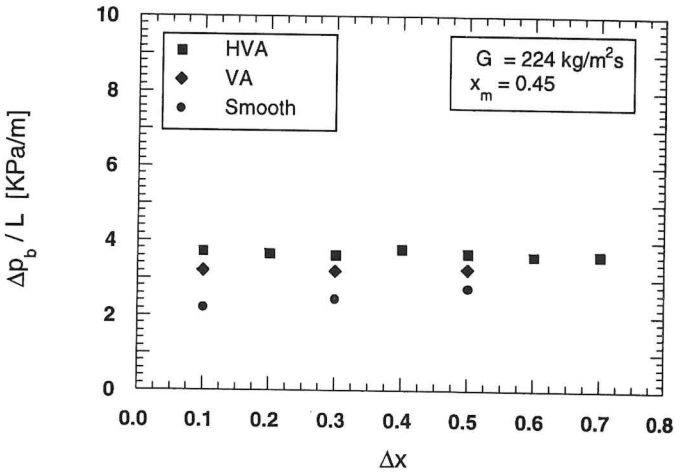

Figure 11. Flow-boiling pressure drop $\Delta p_b/L$ versus quality change Δx for fixed mass flux G and average quality x_m.

increases significantly with mass flux and quality. However, at higher vapour quality pressure drop falls off toward the data point for the vapour phase only pressure drop. Instead, the influence of quality change seems to be negligible. As expected, microfin tubes display pressure drops higher than those of the smooth tube, even if the increment is 44% at the most. Tubes VA and HVA essentially exhibit the same penalty factor -defined as the ratio of pressure drop of a microfin tube to that of the smooth tube- with values varying from 1.44 to 1.13 while G ranges between 160 and 440 kg/sm^2.

Condensation pressure drop for x_{in}=0.8 and x_{out}=0.2 is plotted versus mass flux in Figure 12. As for boiling, pressure drop is an increasing function of G with values, for microfin tubes, larger than those of the smooth tube. Penalty factors, which are practically the same for both the microfin tubes, range from 2.1 to 1.2 for G varying between 130 and 440 kg/sm^2. With reference to the effects of average quality and quality change, the experimental data show that at fixed mass flux and quality change (G=224/238 kg/sm^2 and Δx=0.3) pressure drop increases with average quality varying over the range from 0.3 to 0.7 while, for given mass flux and average quality (G=224/238 kg/sm^2 and x_m=0.5), it is practically insensitive to quality change variation over the range from 0.2 to 0.7.

4. CONCLUSIONS

In-tube evaporation and condensation heat transfer characteristics and pressure drop for R-22 inside two microfin tubes and a smooth tube are reported in this study. All the tubes have outer diameter of 9.52 mm and are horizontally operated. The two microfin tubes differ mainly in the number of fins, i.e., 54 in one case and 82 in the other one.

Conclusions of the present study include:

1. In the range of this study, both microfin tubes exhibit a significant heat transfer enhancement when compared to the smooth tube. The enhancement factors range from 4 to 1.6 for evaporation and from 2.7 to 1.8 for condensation. Furthermore, microfins causes the onset of dryout to be shifted towards higher values of vapour quality because of their hgher capability to keep the wall wet (liquid is conveyed upward).
2. Pressure drop also increases in the microfin tubes but to a lesser extent than heat transfer. In fact, penalty factors

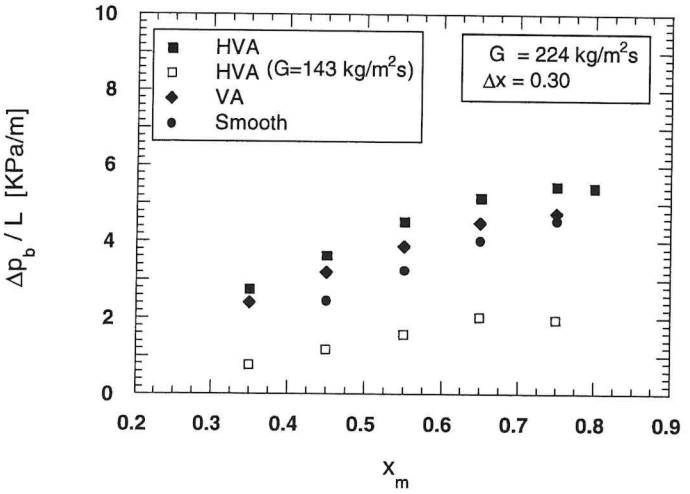

Figure 10. Flow-boiling pressure drop $\Delta p_b/L$ versus average quality x_m for fixed mass flux G and quality change Δx.

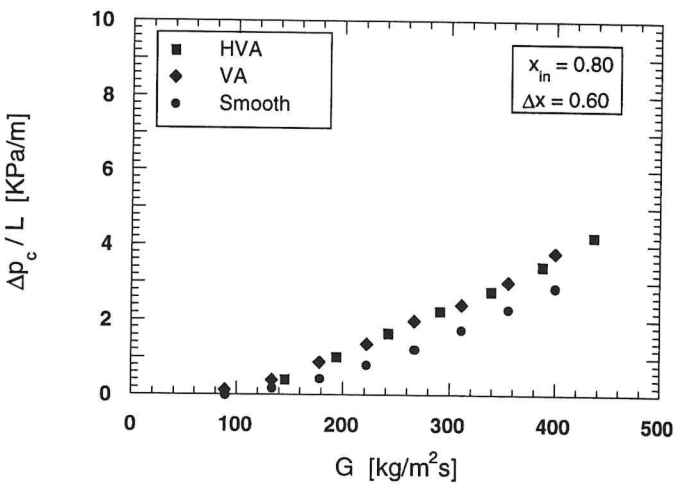

Figure 12 Condensation pressure drop $\Delta p_c/L$ versus mass flux G for fixed inlet quality x_{in} and quality change Δx.

range from 1.44 to 1.13 in evaporation and from 2.1 to 1.2 in condensation

3. Tube VA, that is the tube with 54 fins, appears to show the best heat transfer performance over the range of variables tested both in evaporation and condensation. Penalty factors are practically the same for both microfin tubes.

5. ACKNOWLEDGEMENTS

The authors are in debt with Mr M. Corso of the Politecnico di Milano for the invaluable technical assistance in the setting up the experimental apparatus. This work is supported by MURST via Cofinanziamento 1997 grants.

6. NOMENCLATURE

D = nominal diameter, i.e., at the root of microfins, m
G = mass flux, kg/sm^2
h = heat transfer coefficient, W/m^2K
L= overall length of the test section, m
p = pressure, Pa
q = heat flux, W/m^2
T = temperature, K (or °C)
x = thermodynamic vapour quality
Δp = pressure drop, KPa
Δx = change in thermodynamic quality
ρ = density, kg/m^3

Subscripts

b= boiling
c= condensation
g= vapour phase
i=subsection index
in=entrance of the test section
l = liquid phase
m = arithmetic mean
out=exit of the test section
r = refrigerant
s = saturation condition
w = wall

7. REFERENCES

1. R. L. Webb, *Principles of enhanced heat transfer*, pp. 446-450, John Wiley & Sons, New York, 1993.
2. R. L. Webb, Advances in Modeling Enhanced Heat Transfer Surface, *Heat transfer 1994, Proc. 10th Int'l Heat Transfer Conference,* Vol. 1, pp. 445-459, 1994.
3. J. R. Thome, Two-phase Heat Transfer to New Refrigerants", *Heat transfer 1994, Proc. 10th Int'l Heat Transfer Conference*, Vol. 1, pp. 19-41, 1994.
4. S. G. Kandlikar and T. Raykoff, Predicting flow boiling heat transfer for refrigerants in microfin tubes, *Proc. of 2nd European Thermal-Sciences and 14th UIT National Heat Transfer Conf.*, Vol. 1, pp. 475-482, 1996.
5. L. M. Schlager, Boiling and Condensation in Micro-Fin Tubes, *VKI Lecture Series on Industrial Heat Exchangers*, 1991.
6. A. Muzzio, A. Niro and S. Arosio, Heat transfer and pressure drop during evaporation and condensation of R22 inside 9.52 mm O.D. microfin tubes of different geometries, *Enhanced Heat Transfer*, Vol. 5, pp. 39-52,1998.
7. S. J. Eckels and M.B. Pate, Evaporation heat transfer coefficients for R-22 in micro-fin tubes of different configurations, HTD-Vol. 202, pp. 117-125, 1992.
8. M. Ito and H. Kimura, Boiling Heat Transfer and Pressure Drop in Internal Spiral-Grooved Tubes, *Bulletin of JSME*, Vol. 2, No. 171, pp. 1251-1257, 1979